kind of probe are displayed, together with the energetic penalty that must be paid if the probe group is not in exactly the best place. Moreover, the closeness of the contours indicates what forces the probe would be experiencing and their direction.

The usefulness of energy contours might be diminished if there were many spurious peaks which could mislead the observer. However the present results show that the major features of a predicted interaction can be studied while smaller peaks are automatically filtered out by the contouring procedure. The significance of these major effects may be judged from the figures, but the amount of information on view is easily varied by recontouring at different energy levels. This recontouring is a quick process that does not require another run of programs GRIN and GRID. On the contrary, it can be done while the energy maps are being studied, so that the user directly controls the amount of information that he is considering at any time.

The ability of different probes to interact favorably with proteins appears to follow a general ranking order. It is not uncommon to find sites where the "extended" amino group has a computed energy of −15 kcal/mol, and values as high as −23 kcal/mol have been observed. At the other end of the scale comes the "extended" methyne group (CH), which has a low polarizability and does not hydrogen bond at all. "Extended" methyl (CH_3) is a little better but rarely achieves more than −4 kcal/mol, while carbonyl oxygen may reach −7 and carboxy oxygen −10 kcal/mol. One cannot be precise about the ranking order, and it must be borne in mind that a complete carboxy group contains two oxygen atoms while the computation relates to one alone. Although no quantitative claims should be made for the actual contour levels, these observations suggest that amino and carboxy functions might be used with advantage when high-affinity ligands are being designed.

The present examples mostly come from well-known binding sites on well-known proteins, but contour peaks often indicate favored sites where no ligand other than water has been observed so far. For example, a water molecule has been reported in the pig insulin structure at hydrogen bonding distance from a backbone nitrogen and a backbone carbonyl and Glu-4 Oε1. The highest peak on the contour map for an "extended" amino probe occurs in precisely the same location with a computed energy of −18 kcal/mol, making this the most favored site–probe interaction anywhere on the porcine insulin molecule.

Sites like this, or the hydrophobic pocket illustrate in Figure 9, may be places where one macromolecule makes biologically significant contacts with another in vivo. On the other hand, nature may not use all the favored sites that occur on proteins, but they could still be appropriate targets for novel therapeutic agents. The α-terminal site of hemoglobin[34] may be such an example, and although the choice of energy functions at any one time is always open to improvement, the present contour maps suggest that there really are favored sites on macromolecules and show that energy contours may provide an effective approach to the design of high-affinity ligands as drugs.

Acknowledgment. I thank Professor Sir David Phillips for his support and encouragement. I am greatly indebted to him and to Margaret Adams, Peter Artymiuk, Jane Burridge, Will Gibson, Sheila Gover, Richard Pickersgill, Graham Richards, Neil Rogers, Michael Sternberg, and Garry Taylor for all their suggestions, advice, and help.

Registry No. I, 59-05-2; III, 738-70-5; IV (n = 5), 82830-33-9; H_2O, 7732-18-5; phospholipase-A2, 9001-84-7; dihydrofolate reductase, 9002-03-3; porcine insulin, 12584-58-6.

(34) Beddell, C. R.; Goodford, P. J.; Kneen, G.; White, R. D.; Wilkinson, S.; Wooton, R. *Br. J. Pharmacol.* **1984**, *82*, 397.

Comparative Computer Graphics and Solution Studies of the DNA Interaction of Substituted Anthraquinones Based on Doxorubicin and Mitoxantrone

Suhail A. Islam,[†] Stephen Neidle,[†] Bijukumar M. Gandecha,[§] Malcolm Partridge,[‡] Laurence H. Patterson,[‡] and Jeffrey R. Brown*[§]

Cancer Research Campaign Biomolecular Structure Research Group, Department of Biophysics, King's College, London WC2B 5RL, School of Pharmacy, Leicester Polytechnic, Leicester LE1 9BH, and Department of Pharmaceutical Chemistry, Sunderland Polytechnic, Sunderland SR2 7EE, England. *Received July 19, 1984*

1-[[(Diethylamino)ethyl]amino]- and 1,4-, 1,5-, and 1,8-bis[[(diethylamino)ethyl]amino]anthraquinones are shown to intercalate into DNA. Computer graphics modelling of their intercalation into the self-complementary deoxydinucleoside d(CpG) showed differences in binding properties. While the 1-substituted compound can bind from either groove, the 1,8-disubstituted compound binds with both substituents in the major groove. In the low-energy state of the complex with the 1,5-disubstituted compound, this ligand "straddles" the site with a substituent in each groove—to do this, the compound must bind to a non-base-paired region, so inducing base pairing. The 1,4-compound binds from the major groove; "straddling" is also possible if full minimization of deoxydinucleoside geometry is performed. The differences in binding mode and interaction energies are reflected in the affinities of interaction (1,5- > 1,4- ≫ 1,8- > 1-); also the antiproliferative effects in vitro are in general agreement with this ranking.

Doxorubicin (1) has a wide spectrum of antitumour activity,[1] and although it shows other cellular effects,[2,3] its cytotoxic effect is probably a result of its intercalative interaction with nuclear DNA.[4] This DNA interaction could lead to the cytotoxicity either directly (by inhibition of DNA and RNA synthesis)[5] or indirectly (by causing single or double strand breaks).[6] In an attempt to mimic

[†] University of London.
[‡] Leicester Polytechnic.
[§] Sunderland Polytechnic.

(1) Young, R. C.; Ozols, R. F.; Myers, C. E. *N. Engl. J. Med.* **1976**, *305*, 139.
(2) Moore, H. W.; Czerniak, R. *Med. Chem. Rev.* **1981**, *1*, 249.
(3) Tritton, T. R.; Yee, G.; Wingard, L. B. *Fed. Proc., Fed. Am. Soc. Exp. Biol.* **1983**, *42*, 284.
(4) Brown, J. R. *Prog. Med. Chem.* **1978**, *15*, 125.
(5) DiMarco, A. *Antibiot. Chemother.* **1978**, *23*, 216.

0022-2623/85/1828-0857$01.50/0

Table I. DNA Binding Properties of 4-7

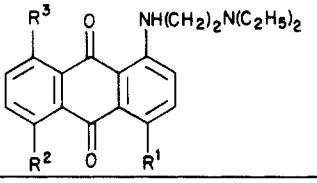

compd	R^1	R^3	R^3	on binding to DNA: shift in λ_{max}, nm	on binding to DNA: % dec in ϵ	ΔT_m,[a] °C	$10^{-6}K$, M^{-1} [b]	n[c]	critical[d] concn, $\mu g\ mL^{-1}$	deg[e]	concn to give 50% ethidium displacement, $M \times 10^6$
4	H	H	H	10	37	8.8	1.48	0.20	0.80	10.6	7.5
5	$NH(CH_2)_2NEt_2$	H	H	20	43	20.0	3.17	0.22	0.16	14.2	0.35
6	H	$NH(CH_2)_2NEt_2$	H	12	27	25.1	3.97	0.21	0.16	14.2	0.85
7	H	H	$NH(CH_2)_2NEt_2$	11	32	9.5	1.71	0.20	0.40	14.3	3.5

[a] The difference between the melting temperature of DNA in the presence and absence of drug at a 10:1 DNA–drug ratio. [b] Affinity constant determined by spectrophotometric titration of drug with DNA. [c] Number of binding sites per DNA phosphate group. [d] The concentration of drug to give comigration of ccc PM-2 DNA with nicked PM-2 DNA under electrophoresis. [e] Degree of unwinding of ccc/DNA per bound drug molecule.

the intercalative properties in simplified derivatives, we prepared a series of anthraquinones,[7] e.g., **2**, and showed that they do indeed bind to DNA.[8] Subsequently mitoxantrone (**3**) has been developed by other research groups and is promising in clinical trial as an antitumor drug.[9-11]

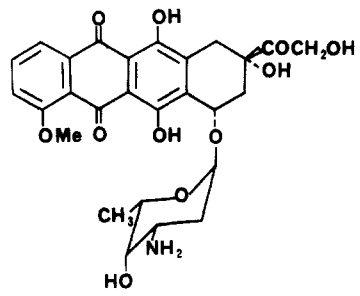

1

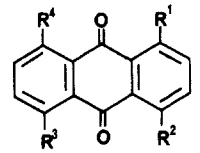

2, $R^1 = R^2 = NHCH(CH_3)(CH_2)_3NEt_2$; $R^3 = R^4 = H$
3, $R^1 = R^2 = NH(CH_2)_2NHCH_2CH_2OH$; $R^3 = R^4 = OH$

As there is now a greater understanding of the DNA-intercalation process for doxorubicin[12,13] and other compounds,[14] we can begin a more rational approach to the engineering of drugs to interact with DNA. In the present study we have evaluated the validity of such an approach.

The results from solution studies on the DNA binding of four (aminoalkyl)amino-substituted anthraquinones (**4–7**, Table I), which differ in the substitution pattern, have been correlated with the results from computer graphics modelling of their fit into a DNA-intercalation site. The data for compound **7** have already been published[15] and serve as a basis for comparison of the series of four compounds.

Synthesis

Compounds **4** and **6** were prepared by reaction of 1-chloroanthraquinone and 1,5-dichloroanthraquinone with 2-(diethylamino)ethylamine.[7] Compound **5** was prepared essentially by the method of Greenhalgh and Hughes[16] by reaction of 2-(diethylamino)ethylamine with leucoquinizarin[7,9-10]. The synthesis of compound **7** has been reported previously.[15] All compounds were prepared as the free base and as the hydrochloride salt.

DNA-Binding Studies

All four compounds showed bathochromic and hypochromic shifts, with an isosbestic point in the visible region of the spectrum, on binding to DNA (Table I). Scatchard plots of the results from spectrophotometric titration of drug with DNA showed the affinity for DNA to be in the order 1,5-compound **6** > 1,4-compound **5** > 1,8-compound **7** > 1-compound **4** (Table I). This order was reflected in the stabilization of DNA to thermal denaturation (Table I) though the 1,4-compound **5** was more effective in displacement of ethidium from its binding sites on DNA than was the 1,5-compound **6**. All compounds were found to unwind ccc-DNA and the degree of unwinding/drug molecule was 10.6° for the monosubstituted compound and 14.2–14.3° for disubstituted compounds. The values are close to those for doxorubicin (11°):[17] and the value for mitoxantrone is 26.5°.[18] The unwinding of DNA, the magnitude of the stabilization of DNA to thermal denaturation, the shifts in the spectra of the drugs, and the displacement of ethidium from DNA binding sites are all consistent with an intercalative binding of these compounds to DNA.

(6) Ross, W. E.; Glaubiger, D.; Kohn, K. W. *Biochim. Biophys. Acta* **1979**, *562*, 41.
(7) Double, J. C.; Brown, J. R. *J. Pharm. Pharmacol.* **1975**, *27*, 502.
(8) Plumbridge, T. W.; Knight, V.; Patel, K. L.; Brown, J. R. *J. Pharm. Pharmacol.* **1980**, *32*, 78.
(9) Murdock, K. C.; Child, R. G.; Fabio, D. F.; Angier, R. B.; Wallace, R. E.; Durr, F. E.; Citarella, R. V. *J. Med. Chem.* **1979**, *22*, 1024.
(10) Zee-Cheng, T. K. Y.; Cheng, C. C. *J. Med. Chem.* **1978**, *21*, 291.
(11) Estey, E. H.; Keating, M. J.; McCredie, K. B.; Bodey, G. P.; Freireich, E. J. *Cancer Treat. Rep.* **1983**, *67*, 389.
(12) Quigley, G. J.; Wang, A. H.-J.; Ughetto, G.; Marel, G.; Van Boom, J. H.; Rich, A. *Proc. Natl. Acad. Sci. U.S.A.* **1980**, *77*, 7204.
(13) Nakata, V.; Hopfinger, A. J. *Biochem. Biophys. Res. Commun.* **1980**, *95*, 583.
(14) Neidle, S.; Abraham, Z. *CRC Crit. Rev. Biochem.* **1984**, *17*, 73.
(15) Islam, S. A.; Neidle, S.; Gandecha, B. M.; Brown, J. R. *Biochem. Pharmacol.* **1983**, *32*, 2801.
(16) Greenhalgh, C. W.; Hughes, N. *J. Chem. Soc. C* **1968**, 1284.
(17) Waring, M. J. *Ann. Rev. Biochem.* **1981**, *50*, 159.
(18) Kapuscinski, J.; Darzynciewicz, Z.; Traganos, F.; Melamed, N. R. *Biochem. Pharmacol.* **1981**, *30*, 231.

Table II. In Vivo Testing against Leukemia P-388[a]

compd	dose, mg kg^{-1}	schedule[b]	T/C
4	16	Q01D×01	95
	8		100
	4		100
	2		98
	1		105
5	128	Q01D×01	111
	64		97
	32		103
	16		112
	8		107
	4		100
	2		95
	1		117
6	128	Q01D×01	92
	64		105
	32		100
	16		105
	8		98
	4		107
	2		98
	1		102
7	8	Q01D×01	107
	4		105
	2		104
	16	Q04D×03	102
	8		98
	4		91

[a] Daunorubicin at 16 mg kg^{-1} on a Q01D×01 schedule gave T/C 143 and at 4 mg kg^{-1} on a Q04D×03 schedule gave T/C 158. [b] Q01D×01 represents a single dose of drug given on day 3 after inoculation. Q04D×03 represents a dosing schedule of a total of three doses with a dosing interval of 4 days (dosing at days, 1, 5, and 9 after inoculation).

Biological Activity

All four compounds were evaluated, as their hydrochloride salts, for activity against P-388 leukaemia in mice. The results are given in Table II. None of the compounds shows any in vivo activity under the conditions used.

The four anthraquinone derivatives were also evaluated for cytotoxic properties by determining (in comparison with doxorubicin) whether they showed an antiproliferative effect against two established cell lines, namely, HeLa and Hep_2. The method used was based on that of Uyeki et al. (1981)[19] with electronic enumeration of cell numbers from harvested monolayers either exposed or not exposed to drug, using a Coulter counter. The results (Table III) show that the disubstituted compounds have an antiproliferative effect vs. Hep_2 cells and that compounds 6 and 7 also are active vs. HeLa cells.

Computerized Model Building

Intercalated double-stranded DNA was modelled by the self-complementary deoxydinucleoside monophosphate d(CpG) with coordinates taken from its intercalation complex with proflavin.[20] Coordinates for substituted anthraquinones 4 and 7 were taken from their crystallographic analyses.[15,21] Those for compounds 5 and 6 were generated by means of standard bond geometry considerations, as were the positions of hydrogen atoms for all four compounds. The crystal structures of 4 and 7 were of the free bases; protonation was simulated at the chain terminal nitrogen atoms.

Table III. Effect of Doxorubicin and the Anthraquinone Derivatives on Proliferation of HeLa and Hep_2 Cells

compd	concn,[a] μM	antiproliferation effect[b] (% number of untreated cells) HeLa	Hep_2
doxorubicin	1.0	52*[d]	56*
4	10.0	96	92
5	1.0	98	88*
6	1.0	75*[c]	64*
7	10.0	64*	84*

[a] Drug concentrations were checked spectrophotometrically immediately before use. [b] Control tubes contained $8.92 \times 10^{-5} \pm 5\%$ Hep_2 cells or $2.35 \times 10^{-5} \pm 4\%$ HeLa cells. [c] At a concentration of 2 μM. [d] Asterisk indicates result significantly different from control when cells were incubated in the absence of drug (see Method section) ($p < 0.001$).

The intercalation complexes studied here have a large number (>30) of intra- and intermolecular degrees of freedom. Systematic exploration of all these translational and rotational spaces is not plausible, and the procedure adopted in this study has been to minimize a discrete number of reasonable starting models, based on the experimentally observed structural data outlined above. This procedure ensures that low-energy structures are located by the computer modelling. These are local global minima in terms of the constraints imposed by the starting framework of the experimentally observed dinucleoside geometry.

The procedure used was to position the anthraquinone chromophore in a plane 3.4-Å midway from and parallel to the C-G base pairs of the dinucleoside duplex dimer, followed by rotational and translational searches within this plane. Once low-energy positions for the chromophore were found, the anthraquinone side chains were then subjected to systematic energy exploration, using a coarse grid of 60° increments for each torsion angle. Minima found in this way were then subjected to a finer (20°) grid search. Checks on the position of the chromophore were then made so as to further optimize the intermolecular fit, prior to total minimization as described below.

All these operations were performed on an interactive computer graphics system (Gresham-Lion Supervisor 214), and the total energy V_{TOT} was computed at each point of movement. $V_{N\text{-}B}$ was defined as

$$V_{TOT} = V_{N\text{-}B} + V_{TORS} + V_{E\text{-}S} + V_{H\text{-}B}$$

where the nonbonded parameters were those used previously by us.[22] Torsional barrier heights in the torsional energy contribution were taken from ref 23. Electrostatic charges were calculated by the CNDO/2 method,[24] and the dielectric constant used was defined as $\epsilon = 1$ for $r_{ij} < 3$ Å, $\epsilon = 0.75 r_{ij} - 1.25$ for 3 Å $< r_{ij} < 7$ Å, and $\epsilon = 4$ for $r_{ij} > 7$ Å, where r_{ij} is the distance between appropriate atoms. Hydrogen-bonding energy ($V_{H\text{-}B}$) was not represented by an explicit term; instead an implicit procedure[25] was adopted, which for hydrogen atoms included only a nonbonded electrostatic term in the energy summation. Low-energy arrangements found in this interactive manner

(19) Uyeki, E. M.; Nishi, A.; Wittick, P. J.; Cheng, C. C. *J. Pharm. Sci.* **1981**, *70*, 1011.
(20) Shieh, H-S.; Berman, H. M.; Dabrow, M.; Neidle, S. *Nucleic Acids Res.* **1981**, *8*, 85.
(21) Almond, P.; Cutbush, S. D.; Islam, S. A.; Kuroda, R.; Neidle, S. *Acta. Crystallogr., Sect. C* **1983**, *C39*, 627.
(22) Islam, S. A.; Neidle, S. *Acta. Crystallogr., Sect. C* **1983**, *C39*, 114.
(23) Hopfinger, A. J. "Conformational Properties of Macromolecules"; Academic Press: New York, 1973.
(24) The computer program used to these calculations was taken from the Quantum Chemistry Program Exchange (No. 281).
(25) Hagler, A.; Huler, E.; Lifson, E. *J. Am. Chem. Soc.* **1974**, *96*, 5319.

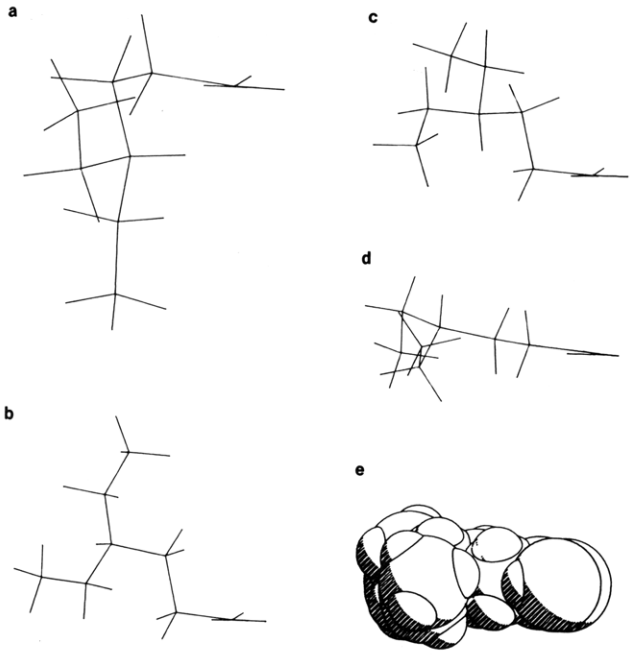

Figure 1. Minimized energy conformations for the (aminoalkyl)amino side chain, corresponding to the energy values given in Table IV. Plot e is a space-filling representation of d.

were subjected to minimization by using the conjugate gradient method[26] with the torsion angles as variables. Although it is known that bond length and particularly bond angle variation may be important factors in helping to stabilize conformations, the present use of a "soft" dispersion potential at least partially compensates for their being maintained at constant values. The alternative would have involved very many more variables in the minimization procedure, with consequently large increases in computational overhead. Convergence of minimization was judged to be complete when the calculated gradient was less than 0.1 kcal mol^{-1}. In general the backbone nucleotide torsion angles altered by no more than 5° during this process. Initial and final torsion angles and coordinates for all the models described are obtainable from S.N.

The conformational flexibility of the (aminoalkyl)amino side chains was also examined as the crystal structures of **4** and **7** indicated that considerable atomic movements were possible.

The Flexibility of the Side Chains. Systematic scans about all the side-chain torsion angles for any isolated side chain at 60° increments (in the absence of dinucleoside) indicated a high degree of flexibility. This was judged by the large number of minima lying within 2 kcal mol^{-1} of the lowest state. A few of these were then minimized. The results are shown in Figure 1a–c and tabulated in Table IV. It is apparent that the flexibility enables the protonated nitrogen atom to adopt positions noncoplanar with the anthraquinone chromophore, maximally ~2.5 Å out of this plane. The terminal methyl groups can extend to ~3.5 Å either side of the plane, so that they can effectively lie in the planes of the base pairs upon intercalation. Figure 1d,e illustrate an attempt to "flatten" the chain. Although of higher energy than Figure 1a–c, the minimum "thickness" can be reduced to ~5.5 Å.

General Topology of Chromophore Intercalation. Figure 2a,b illustrate the two principal categories of drug geometrical disposition in an intercalation site. These are the parallel and perpendicular modes. We have previously shown[15] that, for chromophores not carrying a formal charge, the intermolecular interaction energy with the

(26) Fletcher, R.; Reeves, C. M. *Computer J.* **1969**, *7*, 149.

Table IV. Torsion Angles and Final Energies for Side-Chain Conformations Displayed in Figure 1

	definition of angles			
1	CX	NX1	CX1	CX2
2	NX1	CX1	CX2	NX2
3	CX1	CX2	NX2	CX3
4	CX2	NX2	CX3	CX4
5	NX2	CX2	CX4	HX4A
6	CX2	NX2	CX5	CX6
7	NX2	CX5	CX6	HX6A

	T[f][a]	T[o]	energy of fragments, kcal mol^{-1}
		Figure 1a	
1	−172.98	−122.36	
2	54.52	64.43	
3	49.87	32.71	−19.1
4	166.79	168.16	
5	174.27	174.20	
6	54.29	54.50	
7	51.87	51.60	
		Figure 1b	
1	70.83	59.66	
2	176.89	140.43	
3	53.20	61.73	
4	164.41	168.61	−19.3
5	174.28	174.20	
6	54.53	54.51	
7	59.49	51.61	
		Figure 1c	
1	63.36	59.66	
2	−139.34	−140.57	
3	156.14	159.73	−17.4
4	174.82	168.16	
5	174.05	174.20	
6	54.22	54.51	
7	44.81	51.61	
		Figure 1d	
1	178.08	−179.86	
2	−175.37	−179.70	
3	170.61	165.48	−17.1
4	58.29	58.93	
5	178.18	180.00	
6	100.77	110.44	
7	−178.43	−180.00	

[a] T[o] is the starting and T[f] the final angle in degrees.

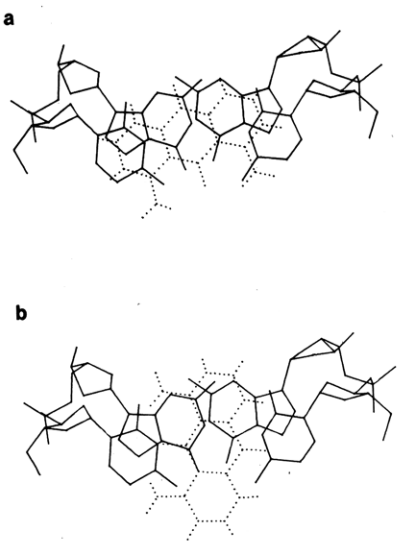

Figure 2. Two principal categories of chromophore intercalation: (a) parallel and (b) perpendicular mode. The chromophore is outlined in dashed lines.

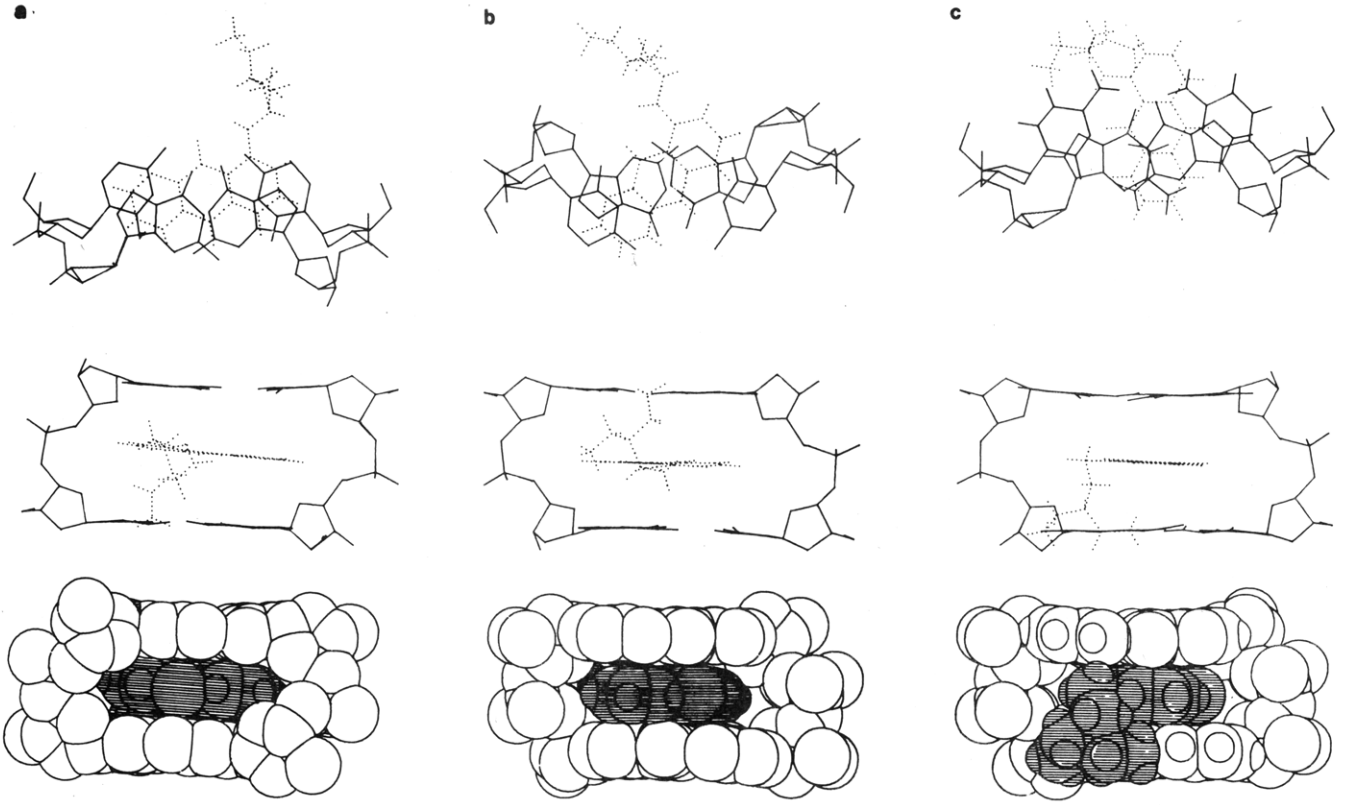

Figure 3. (a) Major groove intercalation of compound **4**. Three computer-drawn views are shown; the top one is perpendicular to the base-pair plane, and the other two are perpendicular to this plane. The bottom plot is a space-filling representation. (b) Minor groove intercalation of compound **4**. (c) Perpendicular mode intercalation of compound **4**.

Table V. Low-Energy States of Anthraquinones 4–7 When Intercalated into the d(CpG) Model for DNA[a,b]

compd	total	V_{N-B}	V_{E-S}	V_{TOR}	V_{H-B}
4 M	−310.2	−188.4	−97.9	5.7	−29.6
4 m	−312.1	−191.9	−97.6	6.9	−29.2
4 P	−305.0	−183.4	−97.3	5.8	−30.1
5	−345.5	−210.9	−109.6	8.3	−33.2
5 S	−373.4	−244.8	−100.5	11.3	−39.4
6	−353.6	−234.0	−97.2	11.2	−33.6
7	−338.2	−212.9	−98.2	7.4	−34.5

[a] Energy values are in kcal mol^{-1}. [b] M, major groove insertions; m, minor groove insertion; P, perpendicular mode; S, "straddling" mode, following full geometry minimization.

nucleic acid is dominated by dispersion forces and that electrostatic interactions play a secondary role. Furthermore, it is the bases rather than the nucleotide backbone that are primarily involved. We estimate that the total intermolecular energy for parallel intercalation of the anthraquinone chromophore shown is −57 kcal mol^{-1} and is 10 kcal mol^{-1} higher for the perpendicular arrangement. The chromophore in both states is able to be moved ±0.5 Å and ±5° from the minimum positions with only small (<1 kcal mol^{-1}) energy changes.

Intercalative Interaction of Anthraquinones 4–7. (i) The 1-substituted compound **4** can be intercalated into d(CpG) from major or minor groove directions. Figure 3a–c show the three low-energy configurations found. The more stable major-groove structure (Table V) has parallel binding, which is similar in energy to the minor groove one. In all these the terminal protonated diethylamino groups interact in a nonspecific manner with the bases and the side chain is free to adopt a number of equally favored conformations.

(ii) The 1,8-substituted derivative **7** can only intercalate from the major groove side, due to steric hindrance in the minor groove. The arrangement is a parallel one. Hydrophobic interaction between the side chains, which is only possible for the 1,8-substituted compound, contributes ~7 kcal mol^{-1} to the total energy and is a factor in their restricted flexibility in this case.

(iii) The 1,5-substituted compound **6** has an enhanced energy of interaction, due to favorable dispersion factors. One side chain resides in the major and the other is in the minor groove. The compound cannot simply be inserted into the intercalation site of d(CpG), since its thickness dimension is minimally ~5.5 Å. This would require an initial base pair–base pair opening of at least 9 Å (5.5 + 3.4 Å). The maximum separation made possible by staggering of backbone conformation is ~8.25 Å.[27] Since intercalative binding is indeed found, the most plausible mechanism for it must involve initial interaction with non-base-paired DNA residues, which subsequently hydrogen bond together. A preference for A-T regions is thus implied, as these have a higher population of transient base-pair disruptions. Dissociation of the 1,5-disubstituted compound **6** from its intercalation site would involve the prior disruption of base pairs not only immediately at but also adjacent to the site. In this case, at least 20–25 kcal mol^{-1} is needed, in addition to the total intermolecular energy of the complex (Table II).

(iv) The 1,4-disubstituted derivative **5** was found to only bind satisfactorily in a perpendicular orientation and having the side chains in the major groove. Minor groove models were subject to unacceptable steric hindrance. This model is of lower energy than the 1- or 1,8-derivatives (**4** and **7**, respectively).

An alternative model with side chains in both grooves, and thus being analogous to the 1,5-disubstituted compound's binding, could be produced only after full geometric minimization of the dinucleoside geometry, with

(27) Miller, K. J.; Macrea, J.; Pycior, J. F. *Polymers* **1980**, *19*, 2067.

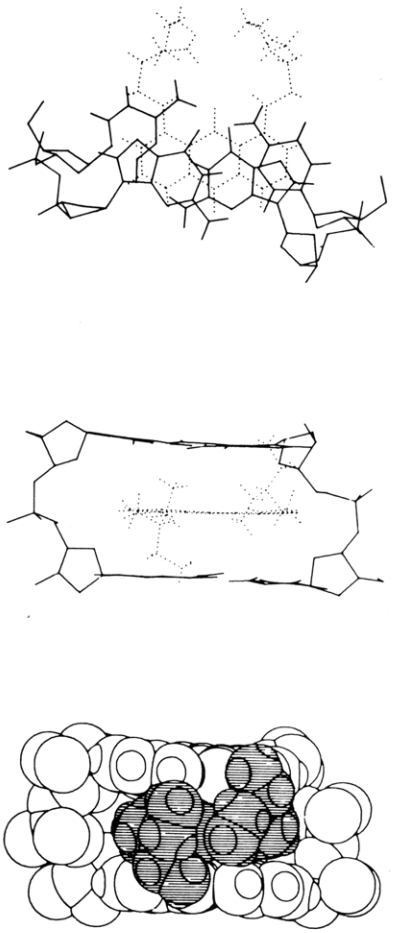

Figure 4. Intercalation model for compound **7**.

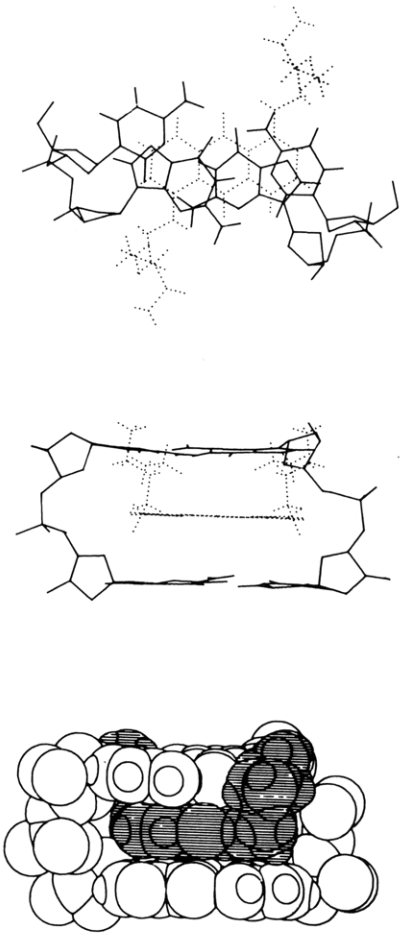

Figure 5. Intercalation model for compound **6**.

bond lengths and angles being optimized.[28] The significant changes in some aspects of the backbone conformations and base-pair hydrogen bonding will be discussed elsewhere. In a qualitative sense, this derivative also requires prior base-pair separation before interaction can take place, and therefore the dissociation energy of the resulting complex is again at least 20–25 kcal mol^{-1} greater than that given in Table II.

Conclusions

This study has shown that the four anthraquinone derivatives studied show large computed variations in their interactions with a model for intercalated DNA, both in terms of geometry and in energy of interaction. They fall into two distinct classes when the property shown by the 1,4- and 1,5-disubstituted compounds **5** and **6**, respectively, of being able to anchor by "straddling" across the intercalation site is taken into account. These two are predicted to bind more strongly to DNA than the 1-substituted and 1,8-disubstituted compounds **4** and **7**, respectively, and moreover to show associated sequence selectivity with a preference for A-T rich regions. These predictions are borne out by the binding data presented in Table III. The overall correlations between V_{TOT}, affinity constants, and ΔT_m values are high (Figure 8) with the best intercalator being the 1,5-disubstituted compound **6**. "Straddling", and hence high stabilization, is the sole mechanism of binding for this compound. Biological measurements of antiproliferative activity are in general, if not absolute,

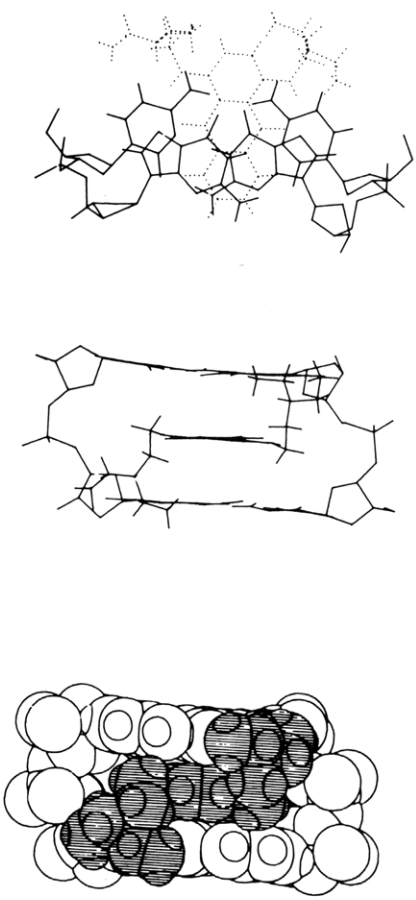

Figure 6. Major groove intercalation for compound **5**.

(28) Performed with the program AMBER (Dearing, A.; Weiner, P. A.; Kollman, P. A. *Nucleic Acids Res.* **1981**, *9*, 1483).

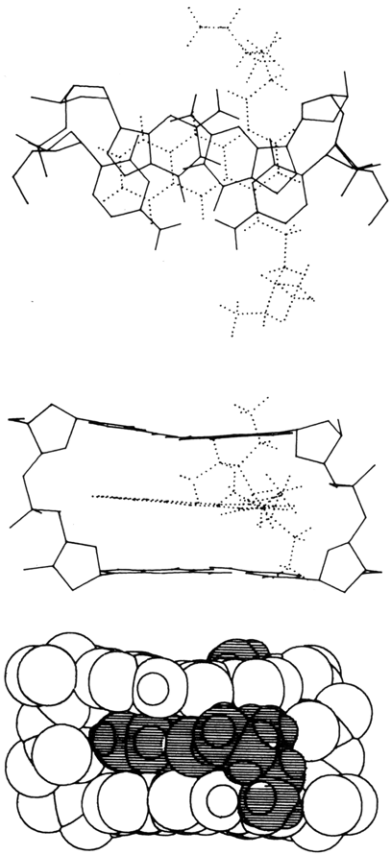

Figure 7. "Straddle" intercalation model for compound **5**.

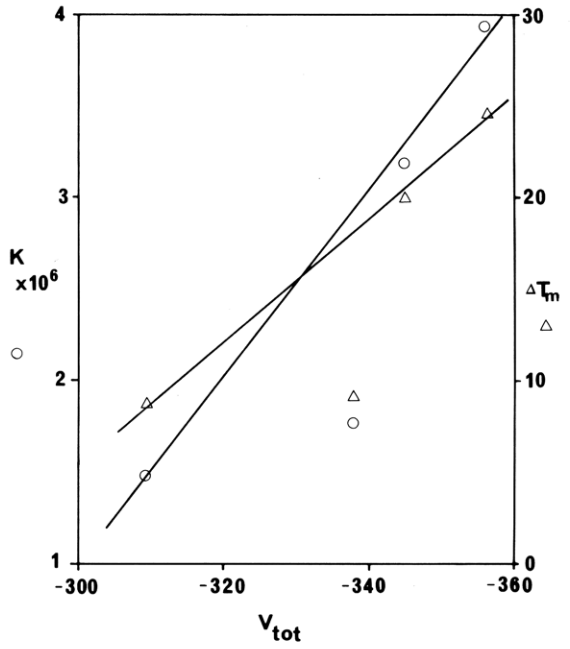

Figure 8. Plot showing relationships for compounds **5–7** between calculated interaction energies (horizontal axis), binding constants, and increase in DNA melting temperature (vertical axes).

agreement with the ranking of the DNA-binding activities from the solution binding studies and from the computer simulations. Certainly the extremes of in vitro behavior for the compounds in the series are consistently indicated with compound **4** being the weakest DNA binder in solution and by theoretical simulation, with **6** being the strongest.

The near-linear relationships in Figure 8 between calculated interaction energy on the one hand and estimations of DNA binding on the other are consistently least well obeyed by the 1,8-derivative. This may be due at least in part to the neglect of entropic contributions to the calculated energy, chiefly from the displacement of solvent by the bound drug. In the case of the 1,8-derivative, its pronounced hydrophobicity in the bound state due to the side chains being on the same side of the molecule could involve qualitatively different solvent environments from those arising with the other derivatives.

These generally high correlations demonstrate that quantitative molecular modelling of drug–DNA intercalation can give reliable comparative estimates of solution binding strengths: further studies from these laboratories will test this hypothesis with other series of DNA-binding drugs.

It is notable that none of the computer simulations indicated any specific drug–base interactions, although it was observed that the terminal methyl could lie in the vicinity of the base planes. Appropriate substitution at these methyl positions could result in participation in specific interactions. We are currently investigating such possibilities.

Experimental Section

All melting points were determined on a Buchi melting point apparatus and are uncorrected. Elemental analyses were carried out by CHN Analysis Ltd., Wigston, Leics., U.K. Where analyses are indicated only by symbols of the elements, analytical results obtained for these elements were within ±0.4% of the theoretical values. A Perkin-Elmer 552-S spectrophotometer, fitted with a temperature programmer, was used for all UV/vis spectrophotometry. Infrared spectra were obtained with a Perkin-Elmer 298 spectrophotometer, NMR spectra were obtained with a Hitachi Perkin-Elmer R 600 (60MHz) NMR spectrometer, and EI mass spectra were obtained with a V.C. Micromass 16F mass spectrometer. A Perkin-Elmer 3000 instrument fitted with a manual polarization accessory was used for fluorimetric analyses. Gel electrophoresis was performed with a Bio-Rad tube electrophoresis apparatus.

1-[[2-(Diethylamino)ethyl]amino]anthracene-9,10-dione (4). 1-Chloroanthraquinone (12.1 g, 0.05 mol; recrystallized from nitrobenzene) was dissolved in 2-(diethylamino)ethylamine (58 g, 0.5 mol) and the solution heated under reflux for 2 h. After the solution cooled, hydrochloric acid (10 N, 100 mL) was added and the mixture extracted with diethyl ether (3 × 200 mL) and then chloroform (3 × 200 mL). The bulked chloroform extracts were dried and evaporated in vacuo, and the residue was dissolved in deionized water. The solution was made alkaline with sodium hydroxide solution and extracted with chloroform (3 × 200 mL). The bulked chloroform extracts were dried and evaporated in vacuo. The residue was washed several times with deionized water, and the last traces of water were removed by addition of absolute alcohol and evaporation in vacuo. The solid was dried over P_2O_5 in vacuo and recrystallized from absolute ethanol: yield 9.67 g (60%); mp 156–158 °C; IR (KBr) 3285 (NH), 3000–2800 (aliphatic), 1660 (CO), 1585 (aromatic) cm^{-1}; UV (0.2 M phosphate buffer, pH 7.0) λ_{max} 248nm (ϵ 16.16 × 10^3), 279 (5.64 × 10^3), 315 (2.99 × 10^3), 495 (3.22 × 10^3); ^1H NMR ($CDCl_3$) δ 7.2–8.3 (7 H, m, aromatic), 3.3 (2 H, t, $ArNCH_2$), 2.6 (6 H, m, CH_2NCH_2), 1.1 (6 H, t, CH_3); EI MS, m/e 322 (M^+). Anal. ($C_{20}H_{22}N_2O_2$) C, H, N.

The hydrochloride salt was prepared by dissolving the free base in the minimum quantity of sodium-dried ether and bubbling dry HCl through the solution; the hydrochloride salt was removed quickly by filtration and stored over P_2O_5 in vacuo.

1,4-Bis[[2-(diethylamino)ethyl]amino]anthracene-9,10-dione (5). Leucoquinizarin (4.84 g, 0.02 mol; recrystallized from acetone–water, 9:1) was suspended in butan-1-ol (100 mL) and 2-(diethylamino)ethylamine (23.2 g, 0.2 mol) added dropwise with stirring under oxygen-free nitrogen. The suspension was heated for 2 h, at 50–55 °C, allowed to stand overnight at room temperature, and then aerated at 50–55 °C. The resultant mixture was evaporated in vacuo and the residue dissolved in hydrochloric acid (2 N, 200 mL). The solution was extracted with diethyl ether

(3 × 200 mL) and then with chloroform (3 × 200 mL), and the extracts were discarded. The aqueous layer was then made alkaline with sodium hydroxide solution and extracted with chloroform (3 × 200 mL). The bulked chloroform extracts were dried and then evaporated in vacuo. The residue was washed several times with deionized water, and the last traces of water were removed by adding absolute ethanol and evaporating in vacuo. The solid was dried over P_2O_5 in vacuo and recrystallized from absolute ethanol: yield 4.88 g (56%); mp 176 °C; IR (KBr) 3420 (NH), 3000–2800 (aliphatic), 1600 (CO), 1585 (aromatic) cm^{-1}; UV (0.2 M phosphate buffer, pH 7.0) λ_{max} 207 nm (ϵ 17.99 × 10^3), 256 (24.72 × 10^3), 582 (9.55 × 10^3), 626 (10.12 × 10^3); ^1H NMR ($CDCl_3$) δ 7.2–8.4 (6 H, m, aromatic), 1.1 (12 H, t, CH_3); EI MS, m/e 436 (M^+). Anal. ($C_{26}H_3N_4O_2$) C, H, N. The hydrochloride salt was prepared as for compound 4.

1,5-Bis[[2-(diethylamino)ethyl]amino]anthracene-9,10-dione (6). This was prepared by the same method as compound 4 with use of 1,5-dichloroanthraquinone (5.52 g, 0.02 mol: recrystallized from toluene) and 2-(diethylamino)ethylamine (23.2 g, 0.2 mol) with heating under reflux for 4 h: yield 4.19 g (48%); mp >300 °C; IR (KBr) 3420 (NH), 3200–2800 (aliphatic), 1660 (CO), 1585 (aromatic) cm^{-1}; UV (0.2 M phosphate buffer, pH 7.0) λ_{max} 201 nm (ϵ 20.17 × 10^3), 231 (31.46 × 10^3), 282 (10.72 × 10^3), 515 (9.50 × 10^3); ^1H NMR ($CDCl_3$) δ 6.8–7.6 (6 H, m, aromatic), 3.4 (4 H, t, Ar NCH_3), 2.7 (12 H, m, CH_2NCH_2), 1.1 (12 H, t, CH_3); EI MS, m/e 436 (M^+). Anal. ($C_{26}H_{36}N_4O_2$) C, H, N. The hydrochloride was prepared as for compound 4.

DNA-Binding Studies. Solutions were prepared in pH 7.4, 0.05 M NaCl, 0.008 M Tris-Cl buffer except where specified otherwise. Calf thymus DNA (Sigma type 1) in buffer was assayed with use of the figure ϵ $(P)_{260}$ = 6600. PM-2 DNA was from Boehringer Mannheim. All compounds obeyed Beer–Lambert's law over the concentration range used. All glassware was silanized before use.

(a) Thermal Denaturation. Drug solution (3 mL) of an appropriate concentration of drug in buffer was added to 600 μL of 2.5 × 10^{-3} M calf thymus DNA in buffer and made up to 10 mL with double-distilled water such that the final solution contained a DNA–drug ratio of precisely 10:1 (in 0.00288 M Tris-Cl, 0.018 M NaCl, pH 7.4 buffer). The absorbance of the solution at 260 nm was recorded as the temperature was raised from 58.0 to 110.0 °C (0.5 °C/min) except for **5** and **6** where absorbance was monitored at the isosbestic point at 268 and 245 nm, respectively. This was repeated for three further samples and the mean T_m calculated. The mean T_m from four similar determinations with DNA in the same buffer in absence of drug was substracted to give the ΔT_m value.

(b) Unwinding Studies with ccc-DNA. PM-2DNA was dissolved in pH 7.4, 0.05 M Tris-Cl buffer containing 0.002 M EDTA, 0.018 M NaCl, and 0.02 M sodium acetate to give a solution of ca. 100 $\mu g\ mL^{-1}$. Appropriate volumes of drug solution (100 $\mu g\ mL^{-1}$) were added to eight 5-mL volumes of 1% Agarose type I (Sigma) in the buffer, at 45 °C, such as to give a range of final concentrations of drug from 0.00 to 1.00 $\mu g\ mL^{-1}$. Each solution was poured into a 125 mm × 5.8 mm glass tube with one end sealed with nescofilm and the ends of the resultant gels trimmed when cool, the nescofilm being replaced with cotton gauze. An aliquot (20 μL) of the PM-2 DNA solution containing drug at a 5:1 molar ratio of DNA phosphate–drug was layered onto the top of the gel followed by 20 μL of 20% sucrose and bromophenol blue. Electrophoresis was performed at 45 V (5 mA/tube) at 20–25 °C for 3–4 h until the bromophenol blue had migrated to about half the length of the gel. The gels were removed, stained with ethidium bromide (4.0 $\mu g\ mL^{-1}$) in the same buffer, destained overnight with the same buffer, and photographed. The critical concentration was determined, this being the concentration at which the ccc-DNA virtually comigrates with nicked PM-2 DNA in the sample.

(c) Determination of Spectral Shifts. Six solutions of drug (2.5 × 10^{-5} M) and DNA were prepared with DNA–drug ratios varying from 0 to 15:1. The spectra were recorded superimposed.

(d) Spectrophotometric Titration. Aliquots (4 × 40, 12 × 20, and 7 × 100 μL) of DNA solution (2.5 × 10^{-3} M) were added sequentially to each of three samples (3 mL) of drug solution (5 × 10^{-5} M), and the absorbance was determined after each addition at the λ_{max} of the unbound drug, after allowing time for equilibration, against a blank of buffer treated in an identical manner. The binding parameters K and n were then determined from a Scatchard plot of (bound drug concentration/DNA concentration)/free drug concentration vs. (bound drug concentration/DNA concentration), the free drug, and bound drug concentrations for each point being determined from the fractional decrease in extinction at that point.

(e) Competition with Ethidium for Binding Sites on DNA. Firstly, aliquots (6 × 10 μL, 5 × 20 μL, 6 × 40 μL, 6 × 100 μL) of a 2 × 10^{-5} M solution of ethidium bromide were added sequentially to a 2-mL volume each of (i) 2 × 10^{-5} M calf thymus in buffer, (ii) 2 × 10^{-5} M calf thymus and 2 × 10^{-6} M drug in buffer, (iii) 2 × 10^{-6} M drug in buffer, and (iv) buffer. The fluorescence of each solution was recorded before and after each addition, at 596 nm (excitation at 476 nm) at 25 °C. Secondly, the fluorescence polarization values of three samples each of six solutions of 2 × 10^{-6} M ethidium bromide and 8 × 10^{-6} M calf thymus DNA containing varying concentrations of drug between 0 and 1 × 10^{-5} M were determined at 596 nm (excitation 476 nm) at 25 °C. The fluorescence polarization of a solution of 2 × 10^{-6} M ethidium bromide in buffer was also determined. The concentration of drug that reduces by 50% the enhancement of the fluorescence polarization of ethidium on binding to DNA was calculated.

Antiproliferative Effects on HeLa and Hep_2 Cells. HeLa cells (Flow Labs., Irvine, Scotland) and Hep_2 cells (Public Health Labs., Leicester Royal Infirmary, Leicester, England) were grown and passaged by using standard techniques essentially as described by Traganos et al.[29] An aliquot (1.0 mL) of cell suspension containing 0.25–1.0 × 10^6 cells mL^{-1} was added to a flat-sided test tube and incubated at 37 °C. After 24 h, medium was changed for fresh medium (controls) or medium containing drug under test. After a further 24-h incubation the surface-adhered cells were detached (using EDTA) and counted electronically with a Coulter counter (Coulter Electronics, Harpenden, Herts, England). Five counts were obtained for each sample, and each data point was the mean of triplicate experiments. Detached cells were shown to be nonviable by the trypan blue exclusion method[29] and the monolayers had a viability of >85% immediately following the EDTA-provoked detachment prior to counting. Doxorubicin was used as a reference compound.

Acknowledgment. The work was supported by the Cancer Research Campaign (grants SP 1384 to S.N. and SP1423 to J.R.B. and a Career Development Award to S.N.). We are grateful to the Cancer Research Campaign Experimental Cancer Chemotherapy Unit, University of Aston in Birmingham for the screening for antitumour activity. S.A.I. is grateful to Professor Peter Kollman for his hospitality and provision of access to his computing facilities.

Registry No. 4, 28843-85-8; 4·HCl, 96259-16-4; 5, 70477-04-2; 5·HCl, 96259-17-5; 6, 1614-59-1; 6·HCl, 96259-18-6; 7, 75312-57-1; 7·HCl, 96259-19-7; 1-chloroanthraquinone, 82-44-0; 2-(diethylamino)ethylamine, 100-36-7; leucoquinizarin, 476-60-8; 1,5-dichloroanthraquinone, 82-46-2.

(29) Traganos, F.; Evenson, D. P.; Staiano-Coico, L.; Darzynkiewicz, Z.; Melamed, M. R. *Cancer Res.* **1980**, *40*, 671.